# Comparison of the electronic structures of the BEDT-TTF4[ M(CN)4] (M = Ni, Pt) and BEDT-TTF4[ M(C2O4)2] (M = Pt, Cu) salts. Structural requirements for hidden Fermi surface nesting

James Martin, Marie-Liesse Doublet, Enric Canadell

Classification
*Physics Abstracts*
71.25P — 71.45L

# Comparison of the electronic structures of the BEDT-$TTF_4[M(CN)_4]$ (M = Ni, Pt) and BEDT-$TTF_4[M(C_2O_4)_2]$ (M = Pt, Cu) salts. Structural requirements for hidden Fermi surface nesting

James D. Martin (*), Marie-Liesse Doublet and Enric Canadell

Laboratoire de Chimie Théorique (CNRS URA 506), Université de Paris-Sud, 91405 Orsay Cedex, France

*(Received 9 June 1993, revised 15 July 1993, accepted 3 August 1993)*

**Abstract.** — The BEDT-$TTF_4[M(CN)_4]$ (M = Ni, Pt) and BEDT-$TTF_4[M(C_2O_4)_2]$ (M = Pt, Cu) salts are metallic at room temperature but exhibit metal-to-semiconductor transitions at lower temperatures. Their electronic structures have been studied by performing tight-binding band structure calculations on their cationic sublattices. All of these salts possess electron and hole Fermi surfaces, in agreement with their metallic character at room temperature. Although the calculated Fermi surfaces for the two series of salts are not very different, the analysis of their crystal structures suggests that the BEDT-$TTF_4[M(C_2O_4)_4]$ (M = Pt, Cu) salts should have a more anisotropic character than the BEDT-$TTF_4[M(CN)_4]$ (M = Ni, Pt) ones. The analogy between the crystal and electronic structures of the BEDT-$TTF_4[M(C_2O_4)_2]$ (M = Pt, Cu) and the BEDT-$TTF_2ReO_4$ salts, and the fact that the shape of the Fermi surface of BEDT-$TTF_4[Pt(CN)_4]$ does not change appreciably when the temperature is lowered, suggest that the metal-to-semiconductor transition is due to a Peierls type mechanism for BEDT-$TTF_4[M(C_2O_4)_2]$ (M = Pt, Cu) but not for BEDT-$TTF_4[M(CN)_4]$ (M = Ni, Pt). The occurrence of a Peierls transition in the BEDT-$TTF_4[M(C_2O_4)_2]$ (M = Pt, Cu) salts is explained in terms of hidden Fermi surface nesting.

Charge transfer salts of the organic donor molecule bis(ethylenedithio)-tetrathiafulvalene (BEDT-TTF, (1)) typically contain slabs of donor molecules separated by layers of anions [1]. The large variety of packing motifs of the BEDT-TTF molecules within the slabs leads to a remarkable diversity in their transport properties and hence these materials have been the focus of intense investigation [1-3]. Since donor — anion interactions largely dictate the BEDT-TTF packing motifs, anions of very different shape and size [1, 3-6] have been employed. Although a majority of these salts have been prepared using monovalent anions, several groups have prepared charge transfer salts of BEDT-TTF and square planar organometallic dianions [7-14].

(*) *Present address :* Ames Laboratory, Iowa State University, Ames, Iowa 50011-3020, U.S.A.

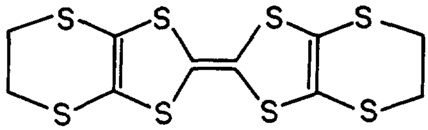

1

BEDT-TTF

Gärtner *et al.* [7] obtained three different BEDT-$TTF_4$[$Pt(CN)_4$] salts. One of them ($\beta$-phase) is metallic at room temperature and near 200 K becomes semiconducting. The other salts ($\gamma$- and $\delta$-phases) are semiconducting. Shibaeva *et al.* [8, 9] reported a BEDT-$TTF_4$[$Pt(CN)_4$] salt which, although it has a slightly different unit cell, is very similar in structure and physical properties to the $\beta$-phase. Later, Fettouhi *et al.* [10] reported a structural refinement of BEDT-$TTF_4$[$Pt(CN)_4$] at 293 K and 135 K, i.e., before and after the metal-to-semiconductor transition. They also suggested that the compounds reported by Gärtner *et al.* [7] and Shibaeva *et al.* [8, 9] were in fact the same. The BEDT-$TTF_4$[$Ni(CN)_4$] salt has also been reported [15] and is very similar in both structural and physical properties to BEDT-$TTF_4$[$Pt(CN)_4$].

The physical properties of the BEDT-$TTF_4$[$M(CN)_4$] (M = Ni, Pt) salts contrast with those of the BEDT-$TTF_4$[$M(C_2O_4)_2$] (M = Pt, Cu) ones. Gärtner *et al.* [16] reported a BEDT-$TTF_4$[$Pt(C_2O_4)_2$] salt which is metallic down to about 60 K where it becomes semiconducting and near 200 K it undergoes a metal-to-metal transition. Recently, Wang *et al.* [17] prepared a 4 : 1 salt with $[Cu(C_2O_4)_2]^{2-}$ which is metallic at room temperature and undergoes a metal-to-semiconductor transition at 65 K after two metal-to-metal transitions at 260 K and 160 K. The crystal structure of this salt is quite similar to that of BEDT-$TTF_4$[$Pt(C_2O_4)_2$] except for the fact that one of the two independent BEDT-TTF molecules in BEDT-$TTF_4$[$Cu(C_2O_4)_2$] was shown to be disordered [18]. The metal-to-semiconductor transition of the BEDT-$TTF_4$[$M(C_2O_4)_2$] (M = Pt, Cu) salts are very sharp in contrast to those of the BEDT-$TTF_4$[$M(CN)_4$] (M = Ni, Pt) salts which are quite broad. This suggests a different mechanism for the metal-to-semiconductor transitions in the two series of salts. We have carried out tight binding band structure calculations [19] for all the above mentioned metallic BEDT-$TTF_4$[$M(CN)_4$] (M = Ni, Pt) and BEDT-$TTF_4$[$M(C_2O_4)_2$] (M = Pt, Cu) salts. Our study suggests that the metal-to-semiconductor transitions in the two series of salts are indeed of different origin and are related to a slight but significant variation in the packing of the BEDT-TTF molecules. Since a detailed study of the difference between the electronic structure of the high and low temperature structures of BEDT-$TTF_4$[$Pt(CN)_4$] has been independently carried out by Rovira and Whangbo [20a], we will not report here this part of our study. After submission of our work, an experimental study of the physical properties of BEDT-$TTF_4$[$Pt(C_2O_4)_2$] has appeared [20b].

## Crystal and electronic structure of BEDT-$TTF_4$[$M(CN)_4$] (M = Ni, Pt) salts.

The BEDT-$TTF_4$[$M(CN)_4$] (M = Ni, Pt) salts exhibit crystal structures where layers of the BEDT-TTF donor molecules alternate with layers of the $M(CN)_4^{2-}$ (M = Ni, Pt) anions. The different anions do not significantly alter the packing of the BEDT-TTF donor layers in these crystal structures [7-10]. A perspective view of a donor molecule layer (in the crystallographic *ac* plane) of BEDT-$TTF_4$[$Ni(CN)_4$] [15a] is shown in figure 1. Each donor molecule of figure 1 is viewed approximately along the direction of its central C = C bond. The repeat unit of this slab contains four donor molecules, pairwise related by centers of inversion, resulting in two symmetry inequivalent molecules. The two different types of BEDT-TTF molecules are distinguished in figure 1 with sulfur atoms represented by filled and empty balls, respectively.

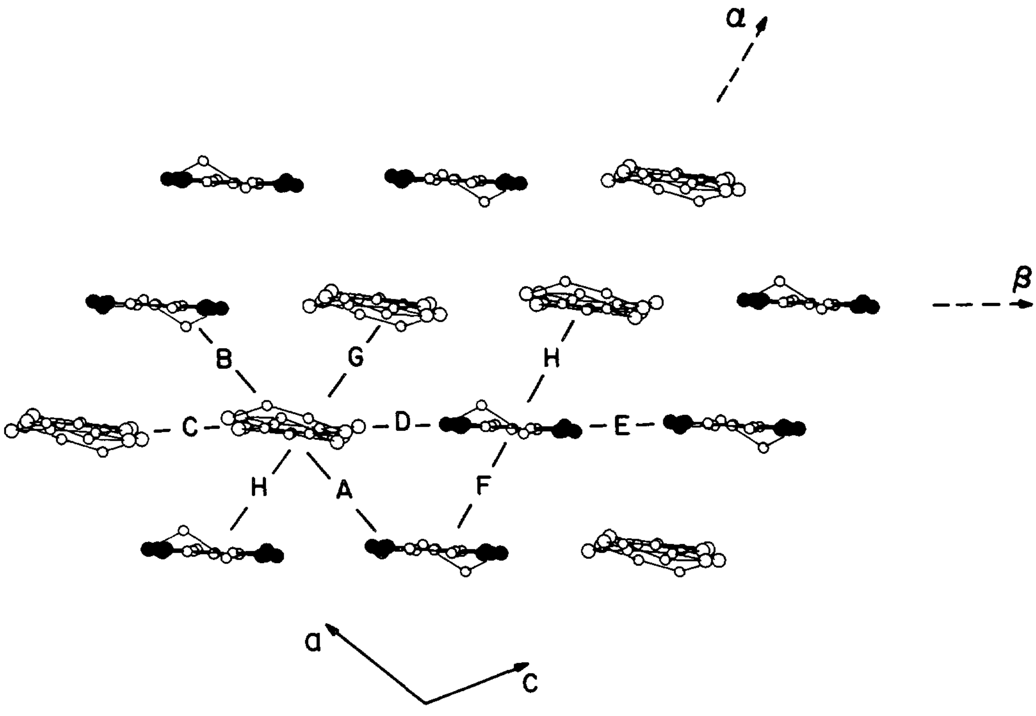


Fig. 1. — Perspective view of a BEDT-TTF layer of BEDT-$TTF_4[Ni(CN)_4]$ [15a]. The hydrogen atoms are not shown for simplicity. Each molecule is viewed approximately along its central C = C bond. The two different types of BEDT-TTF molecules are shown with empty and full sulfur atoms.

Structurally, the slab of figure 1 can be described as a series of inclined columnar type stacks running along a direction between $c$ and $(a + c)$ (the direction $\alpha$ in the Fig.) or as a series of step-chains running along the $a$-crystallographic axis. This stacking arrangement gives rise to eight different types of contacts between donor molecules, designated as A-H in figure 1. Short intermolecular S . S contacts smaller than 3.85 Å (see Tab. I) are observed for both the step

Table I. — S . S *distances smaller than* 3.85 Å *and absolute values of the* $\beta_{\text{HOMO-HOMO}}$ *interaction energies* (eV) *for the different* BEDT-TTF .. BEDT-TTF *interactions in* BEDT-$TTF_4[Ni(CN)_4]$ [15a] *(see Fig.* 1 *for labelling).*

| Interaction type | S ... S distances (Å) | $\beta_{\text{HOMO-HOMO}}$ (eV) |
|---|---|---|
| A | 3.599, 3.692, 3.751, 3.825 | 0.282 |
| B | 3.663, 3.676, 3.721, 3.841 | 0.215 |
| C | 3.446 (× 2), 3.727 (× 2) | 0.156 |
| D | 3.348, 3.376, 3.417, 3.517, 3.830 | 0.142 |
| E | 3.464, 3.604 (× 2) | 0.137 |
| F | 3.812 (× 2) | 0.102 |
| G | (4.144) ([a]) (× 2) | 0.066 |
| H | 3.812, 3.836 | 0.060 |

([a]) Shortest S .. S contact of this interaction type.

chains (...ABAB...) and the columnar stacks (...FHGHF...), as well as for the $\pi$-type chains (...CDEDC.. ) running along the $\beta$ direction in the figure. The two symmetry inequivalent BEDT-TTF molecules have very similar geometries and exhibit central C = C bondlengths of 1.371 and 1.373 Å, respectively, typical [21] of BEDT-TTF$^{+1/2}$ The main difference between these two types of donor molecules is that one of them (those with empty sulfur atoms in Fig. 1) are tilted along their longitudinal molecular axis with respect to those of the other type. This tilting is the result of H ... N hydrogen bonding interactions between one of the two types of BEDT-TTF and the $M(CN)_4^{2-}$ anions.

Because of their nearly identical intramolecular geometries, the energies of the highest occupied molecular orbital (HOMO) of the two different BEDT-TTF molecules are very similar. Thus, the HOMO bands of the slab of donor molecules will result from a strong mixing of the HOMO of both types of molecules. It is possible to estimate the contribution of each of the respective chains to the electronic structure of the donor slab from the corresponding $\beta_{\text{HOMO-HOMO}}$ interaction energies [22] listed in table I. Although the shortest sulfur ... sulfur contacts are those observed along the ..CDEDC.. chain, the $\pi$-type interactions required by this geometric construction result in reduced interaction energies. These interactions are however greater than those of the inclined columnar stacks (.. FHGHF...). The strongest interactions are observed for the step-chains along the $a$-crystallographic axis (.. ABAB.. ). Thus, the BEDT-TTF slabs in BEDT-TTF$_4$[M(CN)$_4$] (M = Ni, Pt) are best described as a series of step-chains along the $a$-direction interacting through weaker $\pi$- and $\sigma$-type contacts in the other directions of the slab.

The calculated band structure and Fermi surface for the BEDT-TTF slabs of BEDT-TTF$_4$[Ni(CN)$_4$] are shown in figures 2a and 2b, respectively. Since the unit cell of the slab contains four BEDT-TTF molecules, there are four HOMO bands. With the formal oxidation required by the stoichiometric formula, (BEDT-TTF)$_4^{2+}$, there are six electrons per unit cell to fill the bands of figure 2a so that the Fermi level (shown by a dashed line in the Fig.) cuts the two upper bands. Thus, the Fermi surface of figure 2b contains electron pockets

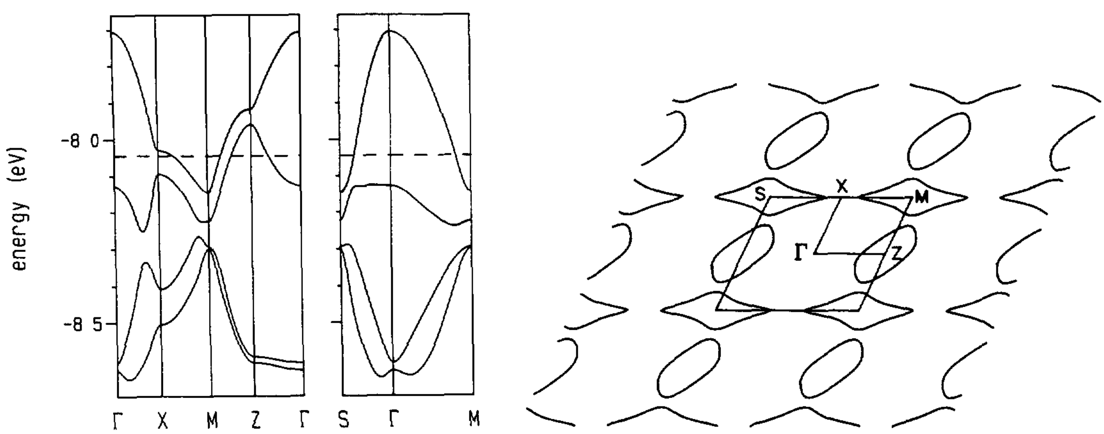


(a) (b)

Fig. 2. — (a) Dispersion relations for the HOMO bands of the BEDT-TTF slabs in BEDT-TTF$_4$[Ni(CN)$_4$], where the dashed line refers to the Fermi level. $\Gamma$, X, Z, M and S refer to (0, 0), ($a^*/2$, 0), (0, $c^*/2$), ($a^*/2$, $c^*/2$) and ($-a^*/2$, $c^*/2$), respectively. (b) Fermi surface associated with the partially filled bands of part a.

centered at M and hole pockets centered at Z. This Fermi surface can be described as a series of « overlapping ellipses » with their short axis slightly off the $a$-direction. Consequently, BEDT-TTF$_4$[Ni(CN)$_4$] should be a two-dimensional (2D) metal with slightly better conductivity along this direction. This is consistent with our analysis of the strength of the different donor-donor interactions on the basis their $\beta$ interactions energies.

Our calculated band structures and Fermi surfaces for the BEDT-TTF layers of BEDT-TTF$_4$[Pt(CN)$_4$] using the crystal structures of Gärtner *et al.* [7], Shibaeva *et al.* [8, 9] as well as the 293 K structure of Fettouhi *et al.* [10] are practically identical. Since band structures are very sensitive to small differences in orientation of the donor molecules because of the strong directionality of the $\pi$-type HOMOs, our results give strong support to the suggestion of Fettouhi *et al.* [10] that the three reported BEDT-TTF$_4$[Pt(CN)$_4$] phases are in fact the same. For our subsequent discussion it is very important to recognize that the Fermi surface of figure 2b is very similar to that calculated with the same method for the room temperature structure of the BEDT-TTF$_2$ReO$_4$ salt [23].

**Crystal and electronic structure of BEDT-TTF$_4$[M(C$_2$O$_4$)$_2$ (M = Pt, Cu) salts.**

The donor layers of BEDT-TTF$_4$[M(C$_2$O$_4$)$_2$] (M = Pt, Cu) [16-18] alternate with layers of isolated M(C$_2$O$_4$)$_2^{2-}$ anions. A perspective view of the donor layers in BEDT-TTF$_4$[Pt(C$_2$O$_4$)$_2$] [16], where each BEDT-TTF molecule is viewed approximately along the central C = C bond, is shown in figure 3. This slab can be described as a series of columnar stacks along the $a$-direction. Every stack is built from two different BEDT-TTF molecules. Because of the presence of inversion centers in between the stacks, the repeat unit of the slab contains two columnar stacks and thus four BEDT-TTF molecules. There are eight different types of donor .. donor interaction types in the layers of figure 3. The different S . . S contacts smaller than 3.8 Å and the corresponding $\beta_{\text{HOMO-HOMO}}$ interaction energies [22] for each of these intermolecular contacts are reported in table II. It is clear that the interactions along the stacks are by far the strongest, and that some of the inter-stack interactions (for instance C, E and G) are extremely weak. It is to be noted that interaction B which is

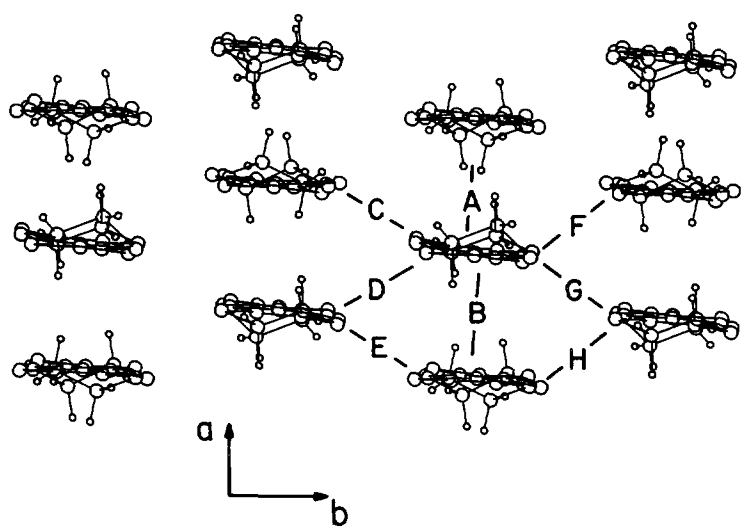


Fig. 3. — Perspective view of a BEDT-TTF layer of BEDT-TTF$_4$[Pt(C$_2$O$_4$)$_2$] [16]. Each molecule is viewed approximately along its central C = C bond.

Table II. — S . S *distances smaller than* 3.8 Å *and absolute values of the* $\beta_{\text{HOMO-HOMO}}$ *interaction energies* (eV) *for the different* BEDT-TTF .. BEDT-TTF *interactions in* BEDT-$TTF_4[Pt(C_2O_4)_2]$ [16] *(see Fig.* 3 *for labelling).*

| Interaction type | S ... S distances (Å) | $\beta_{\text{HOMO-HOMO}}$ (eV) |
|---|---|---|
| A | 3.662, 3.711 (× 2), 3.792 | 0.639 |
| B | (3.905) ([a]) | 0.352 |
| C | 3.511 (× 2), 3.573 (× 2), 3.770 (× 2) | 0.026 |
| D | 3.619, 3.671, 3.673, 3.701, 3.766 | 0.172 |
| E | 3.423 (× 2), 3.624 (× 2) | 0.056 |
| F | 3.651 (× 2), 3.807 (× 2) | 0.177 |
| G | 3.373, 3.382, 3.584, 3.750 | 0.005 |
| H | 3.668 (× 2), 3.716 (× 2) | 0.151 |

([a]) Shortest S .. S contact of this interaction type.

associated with quite long S ... S contacts leads to a strong interaction energy. This is reminiscent of the situation for the BEDT-$TTF_2ReO_4$ salt, whose slabs are quite similar to that of figure 3, and where the strong interaction energies are also associated with some of the interaction types with the longer S ... S contacts [24]. This demonstrates the importance of the orientation of the p-type sulfur orbitals and the need to use overlap integrals (S) or interaction energies ($\beta$) when analyzing the strength of the donor-donor interactions. Our study of BEDT-$TTF_4[Cu(C_2O_4)_2]$ [17, 18] lead to similar results.

The calculated band structure and Fermi surface for the BEDT-TTF slabs of BEDT-$TTF_4[Pt(C_2O_4)_2]$ are shown in figures 4a and 4b, respectively. The four HOMO bands

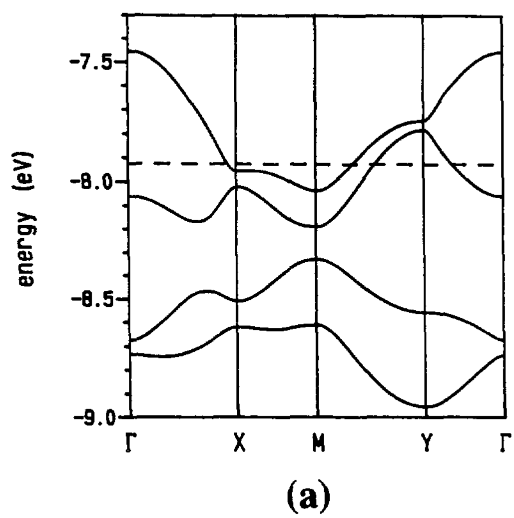


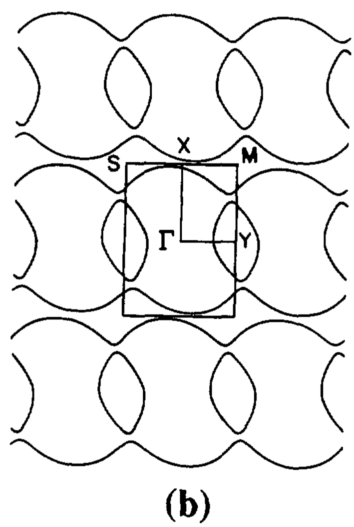


Fig. 4. — (a) Dispersion relations for the HOMO bands of the BEDT-TTF slabs in BEDT-$TTF_4[Pt(C_2O_4)_2]$, where the dashed line refers to the Fermi level. $\Gamma$, X, Y and M refer to (0, 0), ($a^*/2$, 0), (0, $b^*/2$) and ($a^*/2$, $c^*/2$), respectively. (b) Fermi surface associated with the partially filled bands of part a.

result from a strong mixing of the HOMOs of the two types of molecules. With the formal oxidation required by the stoichiometric formula (BEDT-TTF)$_4^{2+}$, there are six electrons per unit cell to fill the bands of figure 4a so that the Fermi level (shown by a dashed line in the Fig.) cuts the two upper bands. Thus the Fermi surface of figure 4b contains both hole and electron pockets. The Fermi surface of the hole pockets is a closed loop centered at Y and hence is 2D in character. The Fermi surface of the electron pockets is open and hence is one-dimensional (1D) in character. Consequently, as suggested by the analysis of its crystal structure, BEDT-TTF$_4$[Pt($C_2O_4$)$_2$] should be a 2D metal but more anisotropic than BEDT-TTF$_4$[Pt(CN)$_4$]. An important observation is that the Fermi surface of figure 4b is very similar to that calculated with the same method for the low temperature (125 K) structure of the BEDT-TTF$_2$ReO$_4$ salt [23].

The Fermi level of figure 4a lies only slightly above the upper band at the X point. Consequently, relatively small changes in the crystal structure could change the shape of the electron Fermi surface from open (1D) to closed (2D) nearby the X point. This seems to be the case for BEDT-TTF$_4$[Cu($C_2O_4$)$_2$] according to our calculations. We suggest that the metal-to-metal transitions (at 260 K and 160 K for BEDT-TTF$_4$[Cu($C_2O_4$)$_2$] [17] and 200 K for BEDT-TTF$_4$[Pt($C_2O_4$)$_4$] [16] before the *metal-to-semiconductor transition* (at 65 K for BEDT-TTF$_4$[Cu($C_2O_4$)$_2$] [17] and 60 K for BEDT-TTF$_4$[Pt($C_2O_4$)$_4$] [16] in these salts are associated with this type of slight changes of the Fermi surface. These modifications, which will affect the conductivity of the salt, are probably brought about by small structural readjustments of the slab, associated with partial disorder in the outer six-membered rings of the donors which change when the temperature is lowered. Disorder in one of the two BEDT-TTF molecules has indeed been found in the room temperature structure of BEDT-TTF$_4$[Cu($C_2O_4$)$_2$] [18]. We believe our suggestion finds support in the very recent study by Tajima *et al.* [20b]. These authors have found that the metal-to-metal transition at 200 K for BEDT-TTF$_4$[Pt($C_2O_4$)$_4$] is associated with the appearance of a superstructure (3 × a) below the transition. Although the hole Fermi surface of this salt (see Fig. 4b) exhibits some flat portions, the corresponding nesting vector is not consistent with a commensurate 3 × a superstructure. Hence, we do not believe that nesting of the Fermi surface is the driving force for the metal-to-metal transitions in BEDT-TTF$_4$[M($C_2O_4$)$_4$] (M = Pt, Cu).

**Comparison of the Fermi surfaces of the BEDT-TTF$_4$[M(CN)$_4$] (M = Ni, Pt) and BEDT-TTF$_4$[M($C_2O_4$)$_2$] (M = Pt, Cu) salts and structural requirements for hidden Fermi surface nesting.**

The Fermi surfaces of figures 2b and 4b are not that different. As noted above small structural modifications could change the electron pocket Fermi surface of figure 4b from 1D to 2D in which case the Fermi surfaces for the two series of salts would be very similar. Furthermore, the Fermi surfaces of figures 2b and 4b are nearly identical to those of the room temperature and low temperature (125 K) structures of the BEDT-TTF$_2$ReO$_4$ salt [23]. This salt contains BEDT-TTF slabs which are composed of parallel stacks of donors very much like those of figure 3. The room temperature Fermi surface of BEDT-TTF$_2$ReO$_4$ is like that of figure 2b, i.e., with 2D electron and hole Fermi surfaces. Lowering the temperature (≈ 125 K) leads to a new Fermi surface similar to that of figure 4b, with a 2D hole Fermi surface but a 1D electron Fermi surface. Finally, at 77 K BEDT-TTF$_2$ReO$_4$ undergoes a metal-to-insulator transition associated with a (1/2, 0, 1/2) structural modulation. Below 77 K the donor stack periodicity is doubled [27], suggesting that the transition results from a Peierls transition. However the Fermi surfaces of BEDT-TTF$_2$ReO$_4$ do not exhibit the 2 $k_f$ nesting vector of 0.5 $a^*$ needed to explain this phase transition as a simple Peierls transition. Recently, these puzzling observations were explained on the basis of the concept of hidden Fermi surface nesting [23]. Hence, on the basis of the similarity of the Fermi surfaces of BEDT-$TTF_2ReO_4$ and those of figures 2b and 4b, the metal-to-semiconductor transitions of both BEDT-$TTF_4[M(CN)_4]$ (M = Ni, Pt) and BEDT-$TTF_4[M(C_2O_4)_2]$ (M = Pt, Cu) could result from a hidden Fermi surface nesting mechanism.

The concept of hidden Fermi surface nesting as applied to BEDT-$TTF_2ReO_4$ [23], is that some weak local structural changes, possibly slight displacements of the BEDT-TTF molecules perpendicular to the stack direction, or slight rotations of the BEDT-TTF molecules, could modify the relative magnitudes of the inter- and intrastack transfer integrals, affecting the dimensionality of the system and ultimately leading to the appearance of the otherwise hidden nesting vector in the low temperature Fermi surfaces. Essential for this scenario is that the energy gained by the CDW structural modulation associated with the hidden nesting more than compensates the energy needed for the reduction of the interstack interactions. Thus, the system will undergo the metal-to-semiconductor transition stabilizing this hidden nesting vector only when the reduction of the interstack interactions can be achieved without a strong energy penalty (i.e., when the system is structurally prepared to readjust the Fermi surface with just minor structural changes). In the following we examine why this is most likely the case for BEDT-$TTF_4[M(C_2O_4)_4]$ (M = Pt, Cu) but not for BEDT-$TTF_4[M(CN)_4]$ (M = Ni, Pt).

The essential differences between the donor slabs of BEDT-$TTF_4[M(CN)_4]$ (M = Ni, Pt) and BEDT-$TTF_4[M(C_2O_4)_2]$ (M = Pt, Cu), as indicated by our analysis of the different types of intermolecular interactions and their $\beta$ integrals, is summarized in figure 5. The principal stacks (symbolized by the bold line in Fig. 5) are of the step-chain type in BEDT-$TTF_4[M(CN)_4]$ (M = Ni, Pt) but of the columnar type in BEDT-$TTF_4[M(C_2O_4)_2]$ (M = Pt, Cu). Careful examination of figures 3 and 5, shows that the different step-chains in BEDT-$TTF_4[M(CN)_4]$ (M = Ni, Pt) are strongly interconnected because of the very nature of these step-chains, and suggests that it is not possible to change the dimensionality of the Fermi surfaces, as required by the hidden nesting mechanism, by minor structural modifications. By contrast, the parallel columnar stacks found in BEDT-$TTF_4[M(C_2O_4)_2]$ (M = Pt, Cu) can readily loose interstack interactions, thus providing the driving force for the hidden nesting mechanism. In other words, the internal structure of the BEDT-TTF slabs seems to be prepared to sustain a hidden nesting type mechanism as the origin for the metal-to-semiconductor transition for BEDT-$TTF_4[M(C_2O_4)_2]$ (M = Pt, Cu) but not for BEDT-$TTF_4[M(CN)_4]$ (M = Ni, Pt). The similarity in structure, temperature of the metal-to-semiconductor transition (65 K for BEDT-$TTF_4[Cu(C_2O_4)_2]$ [17], 60 K for BEDT-$TTF_4[Pt(C_2O_4)_4]$ [16] and 77 K for BEDT-$TTF_2ReO_4$ [25] and the sharp change in the resistivity *vs.* temperature curves at the transition, provides support for our proposal.

The very gradual nature of the transition in the BEDT-$TTF_4[M(CN)_4]$ (M = Ni, Pt) salts and the previous analysis suggest that a hidden nesting mechanism is not at the origin of the transition in this case. Since a low temperature structure is available for BEDT-$TTF_4[Pt(CN)_4]$ [10] we calculated both the room temperature and low temperature structure Fermi surfaces for this salt. The two Fermi surfaces are very similar in shape and look like those of figure 2b with closed electron and hole pockets. The only difference is that the size of the electron and hole pockets is slightly smaller at low temperature. Thus the necessary condition for the occurrence of hidden Fermi surface nesting is not fulfilled in the BEDT-$TTF_4[M(CN)_4]$ (M = Ni, Pt) salts [28]. On the basis of these results the only mechanism which could explain the metal-to-semiconductor transition in the BEDT-$TTF_4[M(CN)_4]$ (M = Ni, Pt) salts is an electronic localization.

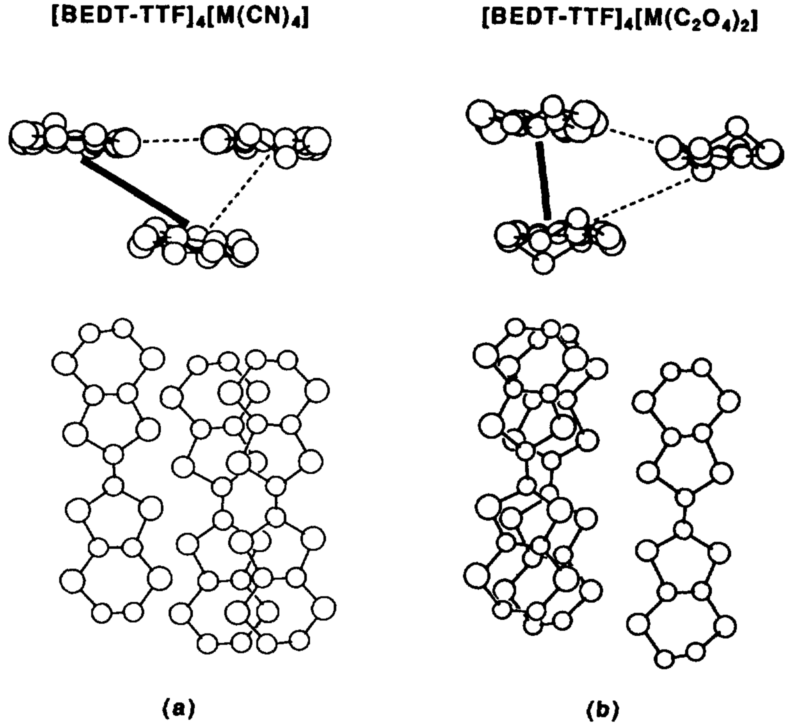


Fig. 5. — Projection views showing the essential differences between the donor networks of (a) BEDT-TTF$_4$[M(CN)$_4$] (M = Ni, Pt), and (b) BEDT-TTF$_4$[M(C$_2$O$_4$)$_2$] (M = Pt, Cu).

**Concluding remarks.**

Tight binding band structure calculations for the room temperature structures of the donor slabs in the BEDT-TTF$_4$[M(CN)$_4$] (M = Ni, Pt) and BEDT-TTF$_4$[M(C$_2$O$_4$)$_2$] (M = Pt, Cu) salts show the existence of electron and hole Fermi surfaces, in agreement with the metallic character of these salts at room temperature. Our calculations for the different structures of the BEDT-TTF$_4$[Pt(CN)$_4$] salt, provides support for the suggestion of Fettouhi *et al.* [10] that the compounds reported by Gärtner *et al.* [7] and Shibaeva *et al.* [8, 9] are in fact the same. Although the Fermi surfaces for the two series of salts are not very different, those of the BEDT-TTF$_4$[M(C$_2$O$_4$)$_2$] (M = Pt, Cu) salts have a greater 1D character than those of the BEDT-TTF$_4$[M(CN)$_4$] (M = Ni, Pt) salts. The shape of the Fermi surface of the BEDT-TTF$_4$[M(CN)$_4$] (M = Ni, Pt) salts is not significantly modified at low temperature. These two facts as well as the analysis of the internal structure of the different BEDT-TTF slabs and the similarity in structure and physical properties of the BEDT-TTF$_4$[M(C$_2$O$_4$)$_2$] (M = Pt, Cu) and BEDT-TTF$_2$ReO$_4$ salts, suggest that a Peierls transition associated with a hidden Fermi surface type mechanism is at the origin of the metal-to-semiconductor transitions in BEDT-TTF$_4$[M(C$_2$O$_4$)$_2$] (M = Pt, Cu) salts but not in the BEDT-TTF$_4$[M(CN)$_4$] (M = Ni, Pt) ones. Electronic localization seems to be the most likely origin for the metal-to-insulator transition in the BEDT-TTF$_4$[M(CN)$_4$] (M = Ni, Pt) salts [20a]. Recently, the concept of hidden nesting has also been found essential to understand the structural instabilities of purple bronzes $AMo_6O_{17}$ (A = K, Na, Tl) [29], Magnéli phases $Mo_4O_{11}$ and monophosphate tungsten bronzes [30], layered transition metal dichalcogenides 1T-$MX_2$ (X = S, Se, Te) [31], $LiVO_2$ [32] and $Sr_3V_2O_7$ [23]. Hence, it would be very important to determine the low temperature structures of the BEDT-$TTF_4[M(C_2O_4)_2]$ (M = Pt, Cu) salts in order to calculate their Fermi surfaces and test the proposed occurrence of hidden Fermi surface nesting in these organic charge transfer salts.

**Acknowledgments.**

We are grateful to D. Schweitzer for sending us the crystal structure of BEDT-$TTF_4[Pt(CN)_4]$ before publication, H. Tajima and M.-H. Whangbo for sending us copies of their work on BEDT-$TTF_4[Pt(C_2O_4)_2]$ and BEDT-$TTF_4[Pt(CN)_4]$, respectively, R. P. Shibaeva for a useful discussion and to one of the referees for pointing out to us the work of reference [20b]. The stay of J. D. M. at Orsay, France, was supported by a postdoctoral grant from the National Science Foundation (Grant No. INT-9007963).

## References

[1] Williams J. M., Ferraro J. R., Thorn R. J., Carlson K. D., Geiser U., Wang H. H., Kini A. M., Whangbo M.-H., Organic Superconductors (Prentice Hall, New Jersey) 1992.

[2] Ishiguro T., Yamaji K., Organic Superconductors (Springer-Verlag, Berlin) 1990.

[3] Williams J. M., Schultz A., Geiser U., Carlson K. D., Kini A. M., Wang H. H., Kwok W.-K., Whangbo M.-H., Schirber J. E., *Science* **251** (1991) 1501.

[4] Urayama H., Yamochi H., Saito G., Sato S., Kawamoto A., Tanaka J., Mori T., Maruyama Y., Inokuchi H., *Chem. Lett.* (1988) 463.

[5] Buranov L. I., Zvarkyna A. V., Kartsovnik M. V., Kushch N. D., Laukhin V. N., Lobkovskaya R. M., Merzhanov V. A., Fedutin L. N., Shibaeva R. P., Yagubskii E. B., *Zh. Eksp. Teor. Fiz.* **92** (1987) 594.

[6] Batail P., Boubekeur K., Davidson A., Fourmigué M., Lenoir C., Livage C., Pénicaud A., The Physics and Chemistry of Organic Superconductors, G. Saito and S. Kagoshima Eds. (Springer-Verlag, Berlin, 1990) p. 353.

[7] Gärtner S., Heinen H., Keller H. J., Niebl R., Nuber B., Schweitzer D., *Z. Naturforsch.* **45b** (1990) 763.

[8] Shibaeva R. P., Lobkovskaya R. M., Korotkov V. B., Kushch N. D., Yagubskii E. B., Makova M. K., *Synth. Met.* **27** (1988) A 457.

[9] Lobkovskaya R. M., Kushch N. D., Shibaeva R. P., Yagubskii E. B., Simonov M. A., *Kristallografiya* **34** (1989) 698.

[10] Fettouhi M., Ouahab L., Grandjean D., Toupet L., *Acta Cryst. B* **48** (1992) 275.

[11] Lobkovskaya R. M., Shibaeva R. P., Kushch N. D., Yagubskii E. B., *Kristallografiya* **35** (1990) 75.

[12] Mori H., Hirabayashi I., Tanaka S., Mori T., Maruyama Y., Inokuchi H., *Solid State Commun.* **80** (1991) 411.

[13] Mori T., Kato K., Maruyama Y., Inokuchi H., Mori H., Hirabayashi I., Tanaka S., *Solid State Commun.* **82** (1992) 177.

[14] Ouahab L., Padiou J., Grandjean D., Garrigou-Lagrange C., Delhaes P., Bencharif M., *Chem. Commun.* (1989) 1038.

[15] (a) Kawamoto A., Tanaka M., Tanaka J., *Bull. Chem. Soc. Jpn* **64** (1991) 3160 ;
(b) Tanaka M., Takeuchi H., Sano M., Enoki T., Suzuki K., Imaeda K., *Bull. Chem. Soc. Jpn* **62** (1989) 1432 ;
(c) Tanaka M., Takeuchi H., Kawamoto A., Tanaka J., Enoki T., Suzuki K., Imaeda K., Inokuchi H., The Physics and Chemistry of Organic Superconductors, G. Saito and S. Kagoshima Eds. (Springer-Verlag, Berlin 1990) p. 298.

[16] Gärtner S., Heinen H., Schweitzer D., Nuber B., Keller H. J., *Synth. Met.* **31** (1989) 199.

[17] Wang P., Bandow S., Maruyama Y., Wang X., Zhu D., *Synth. Met.* **44** (1991) 147.

[18] Qian M., Rudert R., Luger P., Ge C., Wang X., *Acta Cryst. C* **47** (1991) 2358.

[19] Whangbo M.-H., Hoffmann R., *J. Am. Chem. Soc.* **100** (1988) 6093. Our calculations are of the extended Hückel type (Hoffmann R., *J. Chem. Phys.* **39** (1963) 1397) and use a double-$\zeta$ basis set (Clementi E., Roetti C., *At. Nucl. Data Tables* **14** (1974) 177) for all atoms except hydrogen. A modified Wolfsberg-Helmholz formula (Ammeter J., Bürgi H.-B., Thibeault J., Hoffmann R., *J. Am. Chem. Soc.* **100** (1978) 3686) was used to evaluate the nondiagonal $H_{\mu\nu}$ values. The exponents and parameters were taken from : Whangbo M.-H., Williams J. M., Leung P. C. W., Beno M. A., Emge T. M., Wang H. H., Carlson K. D., Crabtree G. W., *J. Am. Chem. Soc.* **107** (1985) 5815.

[20] (a) Rovira C., Whangbo M.-H., *Synth. Met.*, in press ;
(b) Tajima H., Toyoda S., Inokuchi M., Kuroda H., Kobayashi H., *Synth. Met.* **55-57** (1993) 2257.

[21] Beno M. A., Geiser U., Kotska K. L., Wang H. H., Webb K. S., Firestone M. A., Carlson K. D., Nunez L., Whangbo M.-H., Williams J. M., *Inorg. Chem.* **26** (1987) 1912.

[22] (a) Whangbo M.-H., Williams J. M., Leung P. C. W., Beno M. A., Emge T. J., Wang H. H., *Inorg. Chem.* **24** (1985) 3500 ;
(b) Williams J. M., Wang H. H., Emge T. J., Geiser U., Beno M. A., Leung P. C. W., Carlson K. D., Thorn R. J., Schultz A. J., Whangbo M.-H., *Prog. Inorg. Chem.* **35** (1987) 51 ;
(c) Since overlap is explicitely included in extended Hückel calculations, these interaction energies ($\beta$) should not be confused with the conventional transfer integrals ($t$). Although the two quantities are obviously related and have the same physical meaning, the absolute values of $\beta$ are somewhat greater than those of $t$.

[23] Whangbo M.-H., Ren J., Liang W., Canadell E., Pouget J.-P., Ravy S., Williams J. M., Beno M. A., *Inorg. Chem.* **31** (1992) 4169.

[24] Whangbo M.-H., Beno M. A., Leung P. C. W., Emge T. J., Wang H. H., Williams J. M., *Solid State Commun.* **59** (1986) 813.

[25] Parkin S. S. P., Engler E. M., Schumaker R. R., Lagier R., Lee V. Y., Scott J. C., Green R., *Phys. Rev. Lett.* **50** (1983) 270.

[26] Ravy S., Moret, Pouget J. P., Comes R., Parkin S. S. P., *Phys. Rev. B* **33** (1986) 2049.

[27] Ravy S., Moret, Pouget J. P., Comes R., *Synth. Met.* **19** (1987) 237.

[28] For another discussion of the nature of the transition in these salts, see reference [20a].

[29] Whangbo M.-H., Canadell E., Foury P., Pouget J. P., *Science* **252** (1991) 96.

[30] (a) Canadell E., Whangbo M.-H., *Int. J. Mod. Phys. B*, in press ;
(b) Canadell E., Whangbo M.-H., *Phys. Rev. B* **43** (1991) 1894 ;
(c) Canadell E., Whangbo M.-H., *Chem. Rev.* **91** (1991) 965.

[31] Whangbo M.-H., Canadell E., *J. Am. Chem. Soc.* **114** (1992) 9587.

[32] Rovira C., Whangbo M.-H., *Inorg. Chem.*, in press.

# Erratum

## A classification of the periodic directions in the rational approximants of icosahedral quasicrystals

O. Radulescu

*J. Phys. I. France* **3** (1993) 2099-2113

Figure 2 on page 2109 is incorrect. The corrected figure is given below :

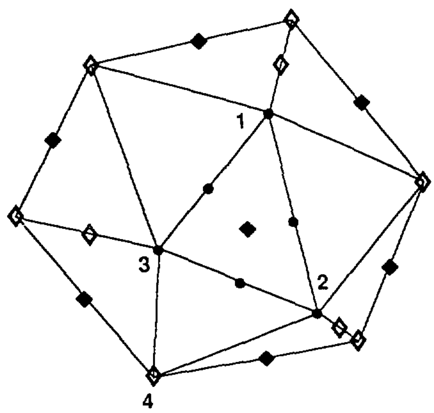

# JOURNAL
# de
# PHYSIQUE
# I

## 1993 AUTHOR INDEX

## VOLUME 3

# Author Index